AD-A143 004 A FLOW VISUALIZATION INVESTIGATION ON SELECTED SHAPES WITH EMPHASIS ON FL..(U) FLORIDA UNIV GAINESVILLE DEPT OF ENGINEERING SCIENCES M H CLARKSON DEC 83 1/1

UNCLASSIFIED AFATL-TR-83-94 F08635-81-K-0201 F/G 20/4 NL

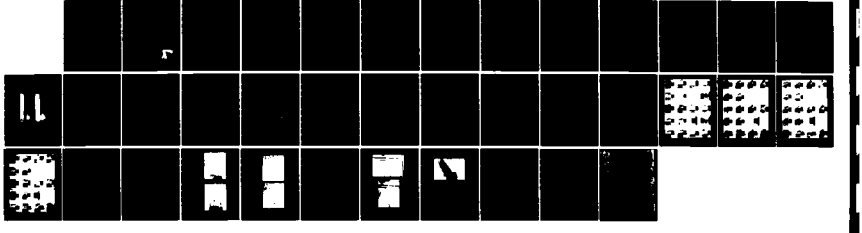

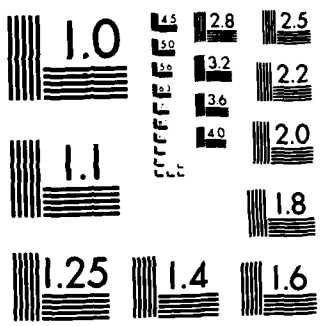

AFATL-TR-83-94

A Flow Visualization Investigation on Selected Shapes with Emphasis on Flow Separation

M H Clarkson

DEPARTMENT OF ENGINEERING SCIENCES
COLLEGE OF ENGINEERING
UNIVERSITY OF FLORIDA
GAINESVILLE, FLORIDA 32611

DECEMBER 1983

FINAL REPORT FOR PERIOD: JULY 1981 - SEPTEMBER 1982

Approved for public release; distribution unlimited

Air Force Armament Laboratory
AIR FORCE SYSTEMS COMMAND★UNITED STATES AIR FORCE★EGLIN AIR FORCE BASE, FLORIDA

NOTICE

Please do not request copies of this report from the Air Force Armament Laboratory. Additional copies may be purchased from:

National Technical Information Service
5285 Port Royal Road
Springfield, Virginia 22161

Federal Government agencies and their contractors registered with Defense Technical Information Center should direct requests for copies of this report to:

Defense Technical Information Center
Cameron Station
Alexandria, Virginia 22314

UNCLASSIFIED

SECURITY CLASSIFICATION OF THIS PAGE (When Data Entered)

REPORT DOCUMENTATION PAGE	READ INSTRUCTIONS BEFORE COMPLETING FORM
1. REPORT NUMBER: AFATL-TR-83-94	2. GOVT ACCESSION NO.: AD-A143 804
3. RECIPIENT'S CATALOG NUMBER:	
4. TITLE (and Subtitle): A FLOW VISUALIZATION INVESTIGATION ON SELECTED SHAPES WITH EMPHASIS ON FLOW SEPARATION	5. TYPE OF REPORT & PERIOD COVERED: Final Report: July 1981-September 1982
	6. PERFORMING ORG. REPORT NUMBER:
7. AUTHOR(s): M. H. Clarkson	8. CONTRACT OR GRANT NUMBER(s): FO8635-81-K-0281
9. PERFORMING ORGANIZATION NAME AND ADDRESS: University of Florida, College of Engineering, Gainesville, Florida 32611	10. PROGRAM ELEMENT, PROJECT, TASK AREA & WORK UNIT NUMBERS: PE: 61102F; JON: 2307-E1-22
11. CONTROLLING OFFICE NAME AND ADDRESS: Air Force Armament Laboratory (DLCA), Armament Division, Eglin Air Force Base, Florida 32542	12. REPORT DATE: December 1983
	13. NUMBER OF PAGES: 34
14. MONITORING AGENCY NAME & ADDRESS (if different from Controlling Office)	15. SECURITY CLASS. (of this report): Unclassified
	15a. DECLASSIFICATION DOWNGRADING SCHEDULE

16. DISTRIBUTION STATEMENT (of this Report)

Approved for Public Release; Distribution Unlimited.

17. DISTRIBUTION STATEMENT (of the abstract entered in Block 20, if different from Report)

18. SUPPLEMENTARY NOTES

Availability of this report is specified on verso of front cover.

19. KEY WORDS (Continue on reverse side if necessary and identify by block number)

Flow Separation
Flow Visualization
Crossflow Planes
Continuous Distribution of Dye Source
Tracer Dye Element

20. ABSTRACT (Continue on reverse side if necessary and identify by block number)

Four bodies having square sections were tested in the University of Florida water tunnel using the method of continuous distribution of dye sources combined with a tracer dye element. Representative photographs are presented in this report along with a topological interpretation of the flow visualization in crossflow planes. The techniques used are described in detail.

DD FORM 1 JAN 73 1473 EDITION OF 1 NOV 65 IS OBSOLETE

UNCLASSIFIED

SECURITY CLASSIFICATION OF THIS PAGE (When Data Entered)

PREFACE

This report was prepared by the Department of Engineering Sciences, College of Engineering, University of Florida, Gainesville, Florida 32611 under Contract F08635-81-K-0281 with the Air Force Armament Laboratory, Armament Division, Eglin Air Force Base, Florida 32542. Mr Charles Cottrell (DLCA) managed the program for the Armament Laboratory. This work was begun in July 1981 and was completed in September 1982.

The Public Affairs Office has reviewed this report, and it is releasable to the National Technical Information Service (NTIS), where it will be available to the general public, including foreign nationals.

This technical report has been reviewed and is approved for publication.

FOR THE COMMANDER

E. C. NEWMAN, Colonel, USAF
Chief, Aeromechanics Division

(The reverse of this page is blank)

TABLE OF CONTENTS

LIST OF FIGURES

LIST OF PLATES

LIST OF TABLES

LIST OF PLATES

LIST OF TABLES

LIST OF SYMBOLS

A_y = projected area, side view

b = model width

$\overline{C}_y$ = side force coefficient

h_b = height of model base

r = corner radius

R_{h_b} = Reynolds number = $\frac{Uh_b}{\nu}$

U = magnitude of the free-stream velocity vector

u,v,w = velocity components along body axis

x,y,z = body axes: x-y parallel to a flat side, x along body axis

α = angle of attack (see Figure 6)

β = angle of sideship (see Figure 6)

ν = kinematic viscosity

σ = total angle of attack (see Figure 6)

ψ = angle of roll about body axis, positive clockwise looking forward (see Figure 6)

SECTION I

INTRODUCTION

The first step toward understanding complex flows very often begins with a visualization of the flow. For some flows, no one method gives a complete picture at the present time.

Oil flows give a picture of the skin friction lines on the surface of a body but need expert interpretation for the external vortical flows at moderate to high angles of attack.

Dye or smoke introduced through ports in the surface of the model is a useful method for displaying major vortex patterns.

The method developed for the work reported on here shows the feeding sheets to the external vortices as well as the flow patterns in the boundary layers that form on the body.

To aid in the interpretation, an old technique used by Prandtl[1] has been utilized to visualize the flow in a plane perpendicular to the axis of the body. Also, a modification[2] of the method used by Allen and Perkins[3] has been used for the same purpose.

Four models were constructed for the subject tests and are described in Section II. These models were geometrically similar to some of those used in oil flow and grid tuft studies performed at the Air Force Academy[4,5,6].

Test procedures are described in Section III, and a discussion of results is presented in Section IV.

SECTION II

DESCRIPTION OF MODELS

Two basic bodies were constructed with each of the bodies being provided with a 2-caliber tangent-ogive sharp nose (as viewed perpendicular to a flat side) and with a modified 2-caliber nose blunted by fairing into a portion of a sphere of 11/16-inch radius. The models were numbered as follows, with "r" denoting corner radius and "b" denoting model width:

Model I	r/b = 0.2	sharp nose
Model II	r/b = 0.2	blunt nose
Model III	r/b = 0	sharp nose
Model IV	r/b = 0	blunt nose

For Model I, the r/b = 0.2 radius was maintained in the nose region. For the blunt nose models, the transition to the blunt nose was faired in, as can be seen in Figure 1.

The models were constructed from aluminum bar stock.

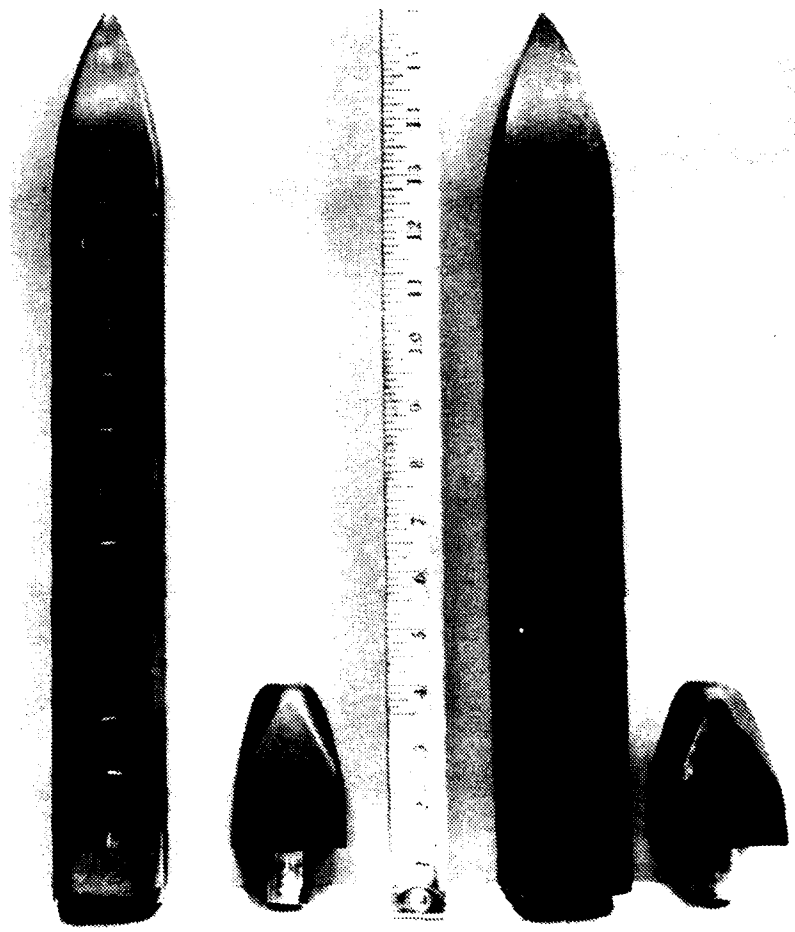

Figure 1. (From Left to Right) Model I, Model II, Model III, and Model IV

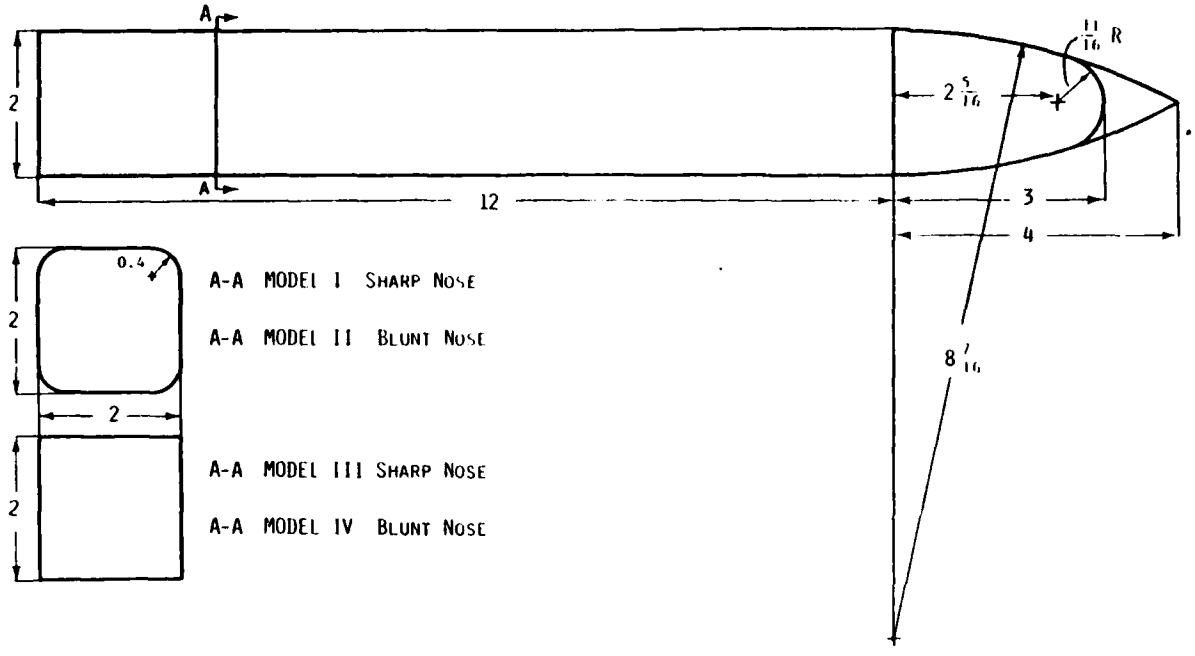

Figure 2. Model Dimensions (in Inches)

SECTION III

TEST PROCEDURES

WATER TUNNEL

The tests were conducted in the University of Florida's water tunnel which is of the flow-down type with flow velocities of about 1 inch per second. The observation time was about 45 seconds. The Reynolds number of the tests was approximately 1000 based on the 2-inch body width. A sketch of the facility is shown in Figure 3.

To view the flow simultaneously from the front and the side, four 16- by 16-inch front surface mirrors were used. The location of these mirrors with respect to the model is shown in Figure 4, and the flow direction and camera angle are displayed in Figure 5.

PHOTOGRAPHIC EQUIPMENT

Two 35-mm Canon cameras were used for the stills. In most cases, a Canon F-1 camera equipped with a Canon motor drive and a Canon data back was used to take color slides using Kodak Ektachrome 160 (tungsten) film. The lens was a Canon 80- to 200-mm zoom lens with a Vivitar 2X giving 160- to 400-mm range of focal lengths. This camera was used with the mirror system. The other Canon camera was used to take three-quarter front views using a 50-mm lens and Kodacolor 400 film. This camera was also fitted with a Canon data back. These data backs have three dials that can be set to put numbers and/or a limited number of characters on the film. These were utilized to indicate [illegible], and model number. The code and parameters tested are given in Table 1. The relations between [illegible] and [illegible] are shown in Figure 6.

Illumination was furnished by three 1000-watt quartz flood lamps located so as to prevent glare and still provide adequate light.

Motion pictures were taken with a Beaulieu 16-mm camera with an Angenieux 17- to 68-mm zoom lens using Kodak video news film (tungsten). The parameters tested are shown in Table 2. Test conditions were listed on a card that was photographed just before each run. The code used was the same as for the still photographs.

FLOW VISUALIZATION

The flow visualization method used in these tests evolved over a period of several years. The original method utilized conventional dye ports. Drawbacks to this method include possible interference between the dye jet and the flow, difficulties in regulating the dye rate in a flow-down facility where the static pressure is changing with time, and, since the number of dye ports is limited, the

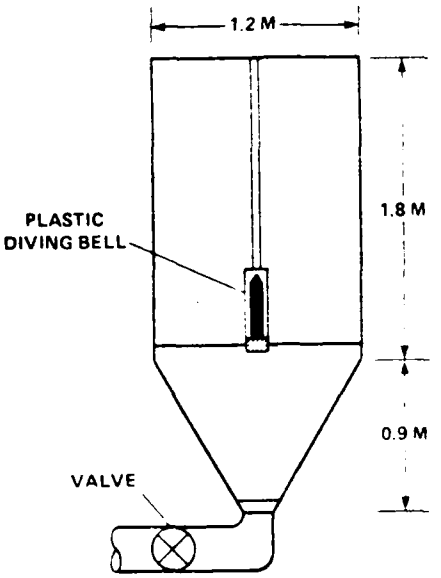

Figure 3. Sketch of the Water Tunnel With a Model Mounted Under the Diving Bell

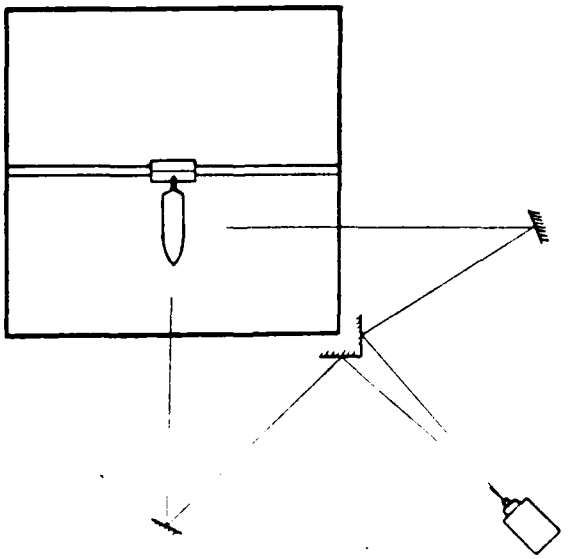

Figure 4. Sketch Showing the Location of the Mirrors and the Camera for Taking Photographs of the Front and Side Views Simultaneously

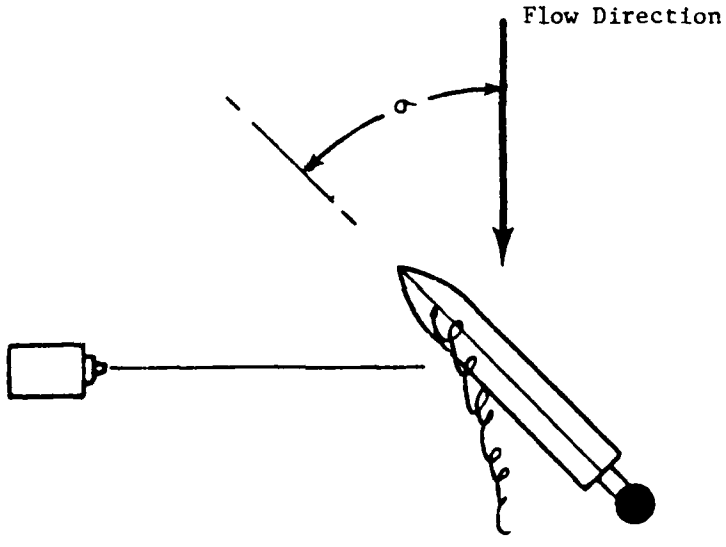

Figure 5. Camera Angle and Flow Direction for Plates I Through IV

TABLE 1. TEST SCHEDULE FOR STILL PHOTOGRAPHS (COLOR SLIDES)

MODEL	TOTAL ANGLE OF ATTACK $\sigma \sim$ deg	ROLL ANGLE $\psi \sim$ deg	CODE
M = I, II,	15	0	1-0-M
III, and IV	15	11	1-1-M
(see below)	15	$22^1/2$	1-2-M
	15	33	1-3-M
	25	0	2-0-M
	25	11	2-1-M
	25	$22^1/2$	2-2-M
	25	33	2-3-M
	25	45	2-4-M
	45	0	4-0-M
	45	$22^1/2$	4-2-M
	45	45	4-4-M
	60	0	6-0-M
	60	$22^1/2$	6-2-M
	60	45	6-4-M

M = I ----- Rounded corners, r/b = 0.2, sharp nose

M = II ---- Rounded corners, r/b = 0.2, sharp nose

M = III --- Square corners, r/b = 0, sharp nose

M = IV ---- Square corners, r/b = 0, sharp nose

Example: 1-0-I, $\sigma = 15°$, $\psi = 0°$, Model I.

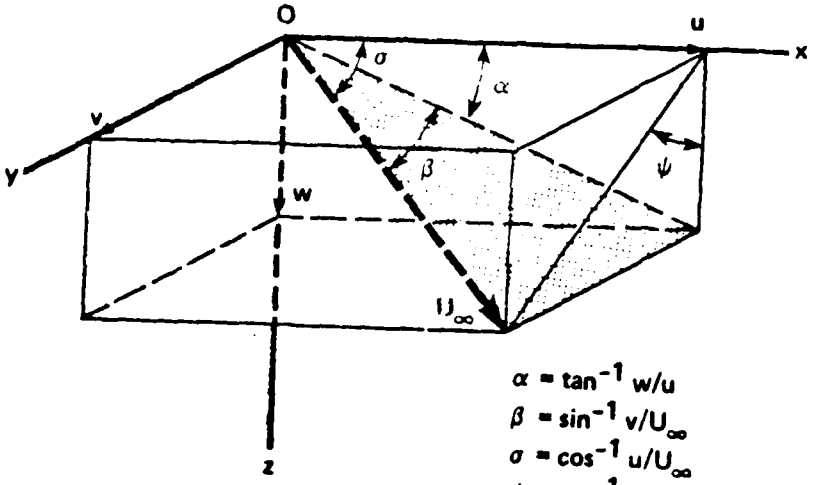

$\alpha = \tan^{-1} w/u$

$\beta = \sin^{-1} v/U_\infty$

$\sigma = \cos^{-1} u/U_\infty$

$\psi = \tan^{-1} v/w$

AND $\tan \psi = \tan \beta / \sin \alpha$

$\cos \sigma = \cos \beta \cos \alpha$

Figure 6. Relations Between [illegible] and [illegible] and [illegible]. [illegible] = [illegible] = 0 when a flat side is horizontal and body axis is parallel to the flow.

TABLE 2. TEST SCHEDULE FOR 16-MM MOVIES

MODEL	σ	ψ	CODE
I	25	0	2-0-I
I	25	45	2-4-I
I	45	0	4-0-I
I	45	45	4-4-I
II	45	0	4-0-II
III	25	0	2-0-III
III	45	0	4-0-III
III	45	45	4-4-III
IV	25	0	2-0-IV
IV	25	45	2-4-IV
IV	45	0	4-0-IV
IV	45	45	4-4-IV

Model I ----- r/b = 0.2, sharp nose

Model II ---- r/b = 0.2, blunt nose

Model III --- r/b = 0, sharp nose

Model IV ---- r/b = 0, blunt nose

σ = total angle of attack = the angle between the body longitudinal axis and the free stream velocity vector (see Figure 6).

ψ = roll angle about the body longitudinal axis, positive clockwise looking forward.

amount of information to be gained is thereby also limited.

The method of a continuous distribution of dye sources was first reported in Reference 7. The idea behind this approach was to provide a more complete visualization of separated flows and, in particular, of the flow separation lines and vortex feeding sheets. In this technique, the model was wetted with hairspray and fluorescein dye powder sprinkled onto the model. A number of methods was tried to keep the model dry until the tank was filled and ready for testing. Plastic bags were fitted around the model in the earlier attempts, but leaks always developed. The diving bell technique proved to be satisfactory and is the method that was used in the subject tests. The diving bell was made from a plexiglass tube and was plugged at the upper end with a half-inch water pipe threaded into the plug. The pipe served as a handle to place the cylinder to keep the water from getting to the model. The pressure supply hose was fitted with a quick opening valve that was opened as the cylinder was removed from the model to prevent unwanted dye from obscuring the model.

In the tests, the flow-down was started as soon as the bell was removed, and photographs were taken after the flow had traveled about two body lengths.

A main result of this technique was to prove experimentally the existence of an open type of separation on a tangent-ogive body with a circular cross section

With the above technique, it is difficult to tell the direction of flow, particularly near the surface. To add this feature to the flow visualization, powdered crystals of methyl violet (gentian violet) were distributed on the model after the sodium fluorescein powder had been applied. A number of other substances was tried. The only other substance which worked was methyl blue. However, methyl violet was considered superior.

To improve repeatability, a concentrated solution of sodium fluorescein, about 50 percent powder, 40 percent water, and 10 percent ethyl alcohol, was painted on the models and methyl violet crystals were then sprinkled onto the still-wet surface. This was the technique followed for all the production runs of this investigation.

SECTION IV

DISCUSSION OF RESULTS

For non-circular shapes, particularly those with corner radii r/b <0.5, the forces and moments are very dependent on nose shape and Reynolds number. The large variations that can occur are amply illustrated in Figure 7 where side force is plotted against Reynolds number for three different models with square cross sections, r/b = 0.25. These data were obtained in the NASA Ames 12-Foot Pressure Tunnel[8]. In light of this type of behavior, the question might well be raised about the value of flow visualization carried out at low Reynolds numbers. The answer is that they have value in at least three ways: (1) They aid in interpreting oil flows where the Reynolds numbers are low. (2) They aid in settling topological questions that can then be applied at higher Reynolds numbers. (3) The gross features are likely to be very close to those of flows at higher Reynolds numbers since the location of the primary line of separation is generally on the corner. This line is certainly on the corner for the sharp cornered bodies at γ = 0° and 45°.

Plates I, II, III, and IV have been prepared to show the effects of [illegible] on Models I, II, III, and IV, respectively. In each of these plates, γ varies from 0° to 45° reading from left to right, and σ varies from 15° to 60° reading from top to bottom, as shown on the facing page of each plate. As the photographs were taken with a zoom lens, not all of those selected for these plates were taken at the same focal length.

To aid in the interpretation of the water tunnel picture, Figures 8, 9, and 10 have been taken from Reference 9 and Figures 11, 12, and 13 have been taken from Reference 10.

The sketches from Reference 9 were deduced from oil flows performed in the wind tunnel at the Air Force Academy and from the water tunnel experiment at the University of Florida. The photographs from Reference 2 are of two types: Figures 11 and 12 were from Model I three quarters submerged and then impulsively started from the rest, and Figure 13 shows two photographs in a sequence from Model I plunging vertically and moving forward horizontally so as to give a γ of 45°. The fuzzy streaks in the first model are due to camera vibration.

Figure 8 shows the variation of the cross flow topology aft of the tangency point and should be compared with Plate III reading across for rows 1 and 2. However, at the resolution possible in the photographs, Figure 8 would apply to Plate I as well and also to Plates III and IV except in the nose region. For Figure 9, Plate III should be read vertically downward in Column 1. Again, the first column of Plate I looks quite similar to Plate III as do Plates II and IV except near the nose. For Figure 10, Plate III should be read vertically downward in Column 5.

Asymmetric vortex flow is noticeable for both sharp noses at γ = 0°, γ = 15° and γ = 25° in Plates I and at γ = 15° in Plate III. This type of flow pattern seems to be typical for sharp-nosed bodies in this angle of attack range, but it is rather unexpected for the sharp-cornered model.

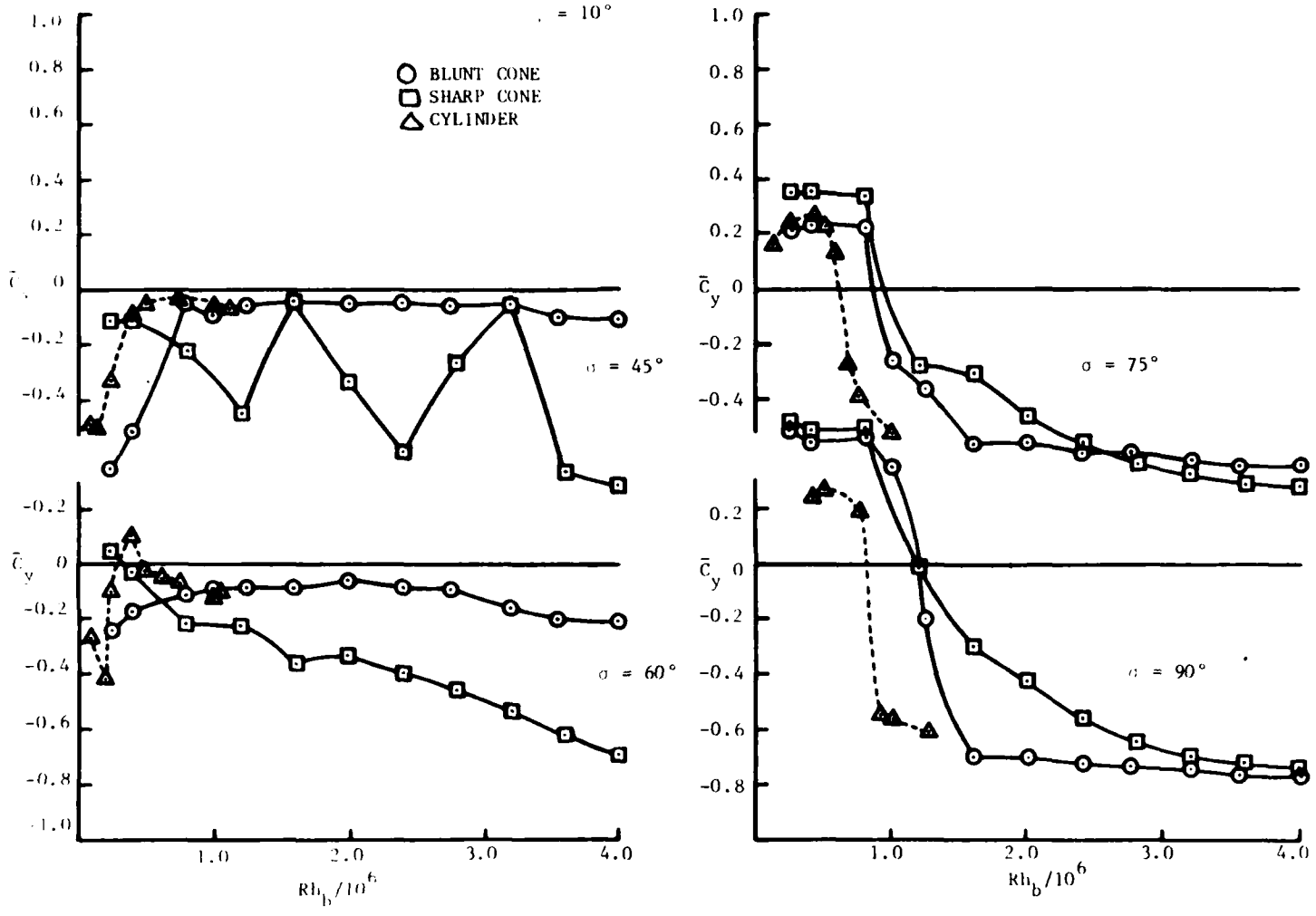

Figure 7. $\bar{C}_y$ Versus Rh_b, Square Cross Section, r/b = 0.25


PLATE I
MODEL I
σ, ψ in degrees

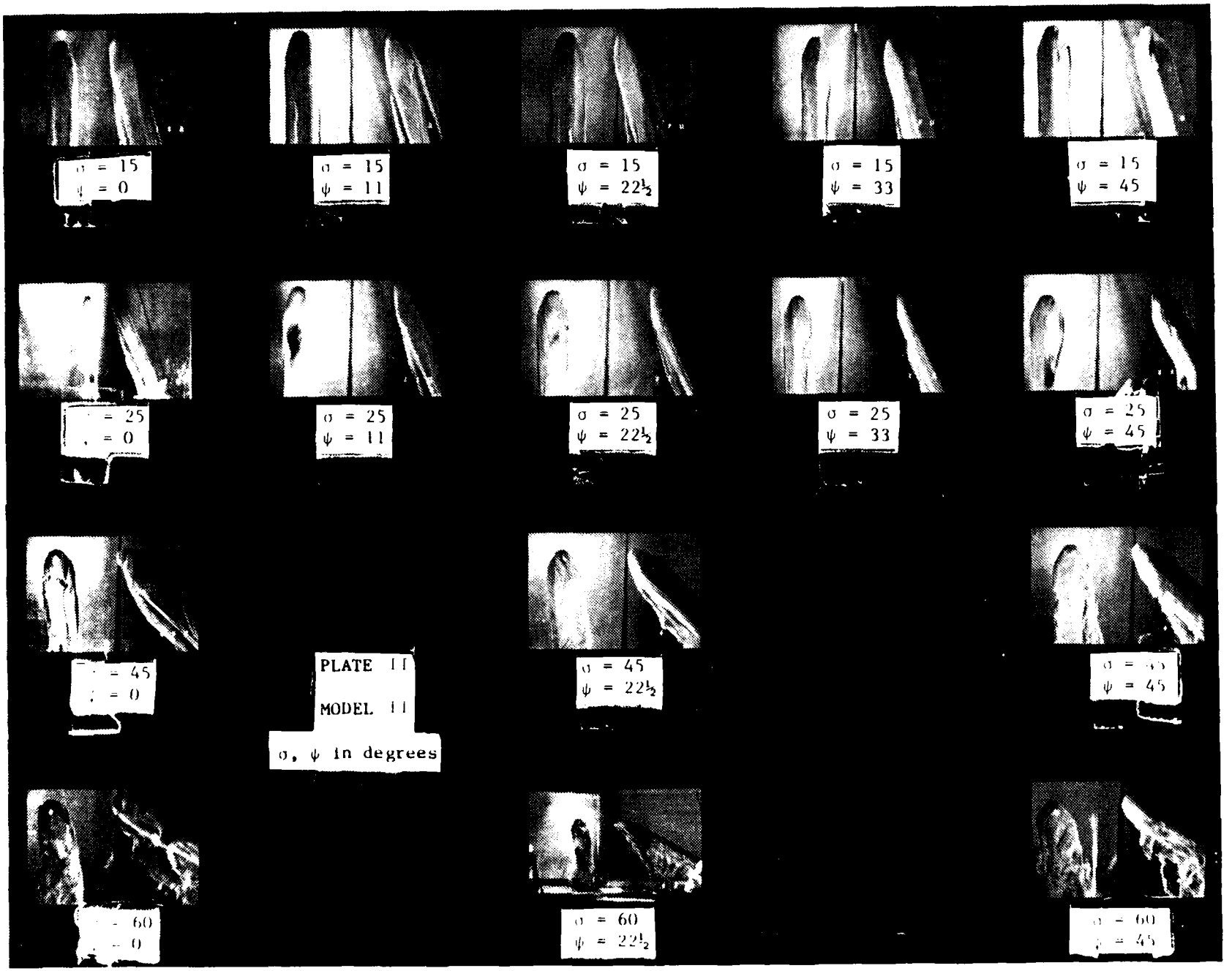
σ = 15
ψ = 0
σ = 15
ψ = 11
σ = 15
ψ = 22½
σ = 15
ψ = 33
σ = 15
ψ = 45
= 25
= 0
σ = 25
ψ = 11
σ = 25
ψ = 22½
σ = 25
ψ = 33
σ = 25
ψ = 45
= 45
= 0
PLATE II
MODEL II
σ, ψ in degrees
σ = 45
ψ = 22½
σ = 45
ψ = 45
= 60
= 0
σ = 60
ψ = 22½
σ = 60
= 45

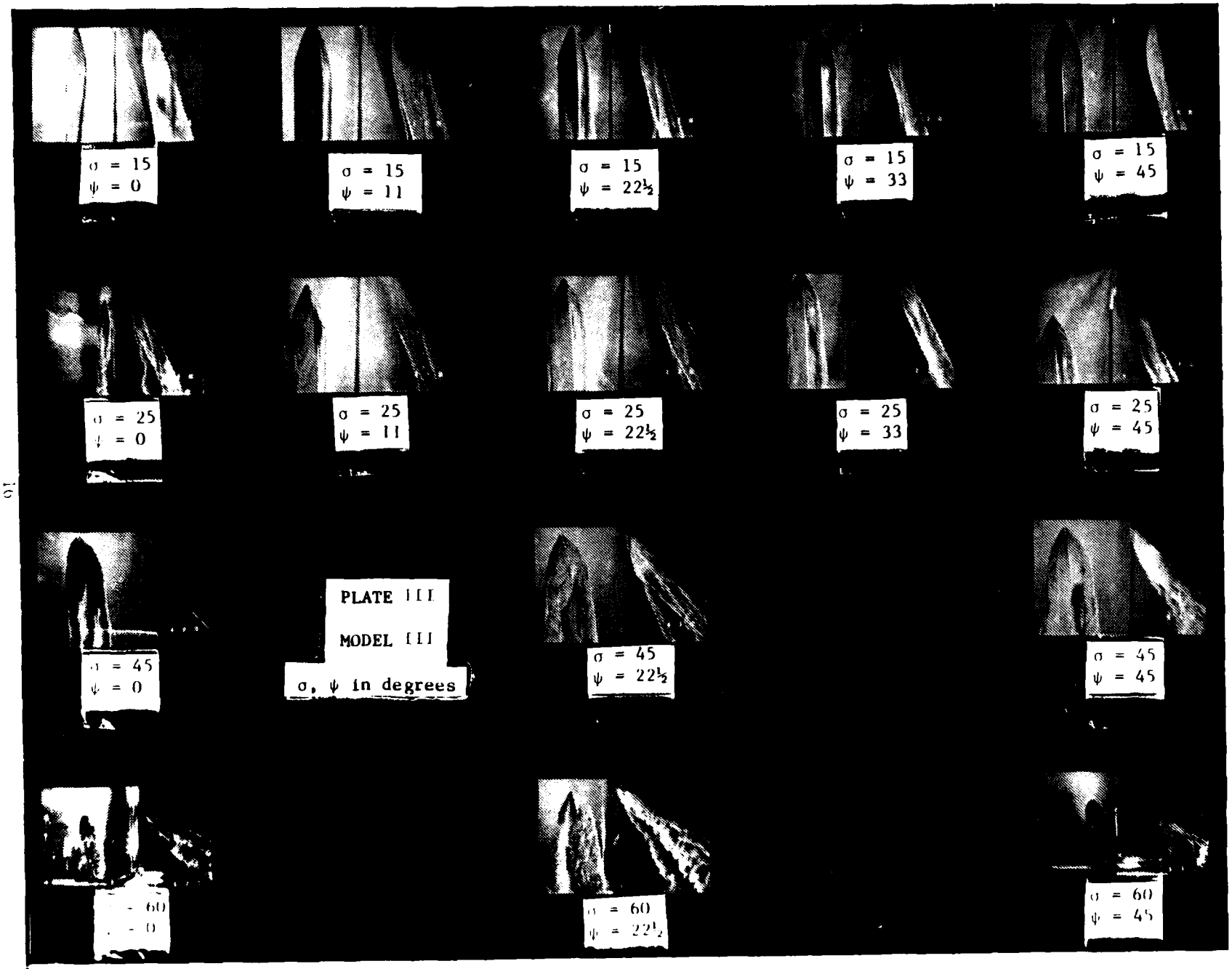
σ = 15
ψ = 0
σ = 15
ψ = 11
σ = 15
ψ = 22½
σ = 15
ψ = 33
σ = 15
ψ = 45
σ = 25
ψ = 0
σ = 25
ψ = 11
σ = 25
ψ = 22½
σ = 25
ψ = 33
σ = 25
ψ = 45
σ = 45
ψ = 0
PLATE III
MODEL III
σ, ψ in degrees
σ = 45
ψ = 22½
σ = 45
ψ = 45
σ = 60
ψ = 0
σ = 60
ψ = 22½
σ = 60
ψ = 45

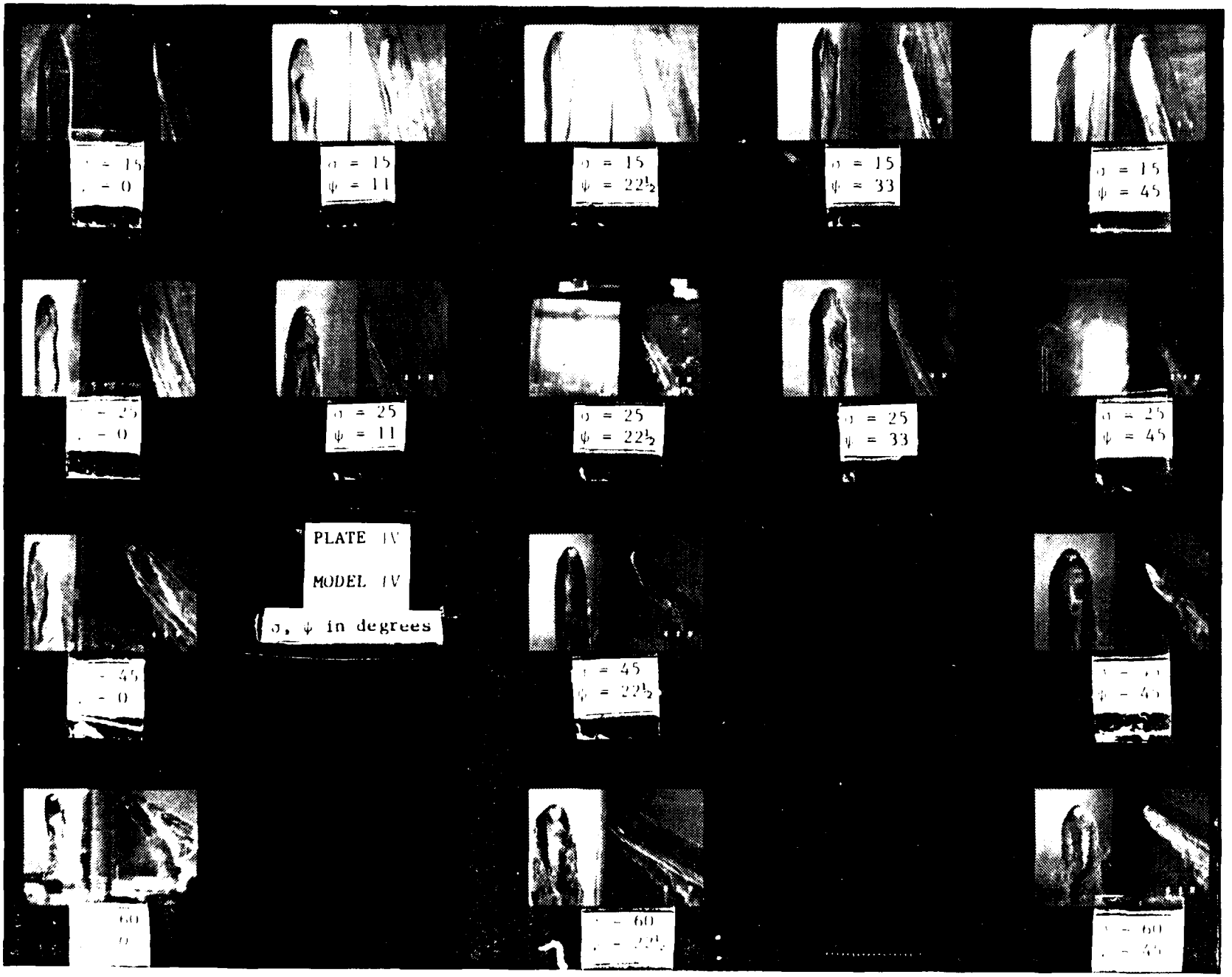
PLATE IV
MODEL IV
σ, ψ in degrees

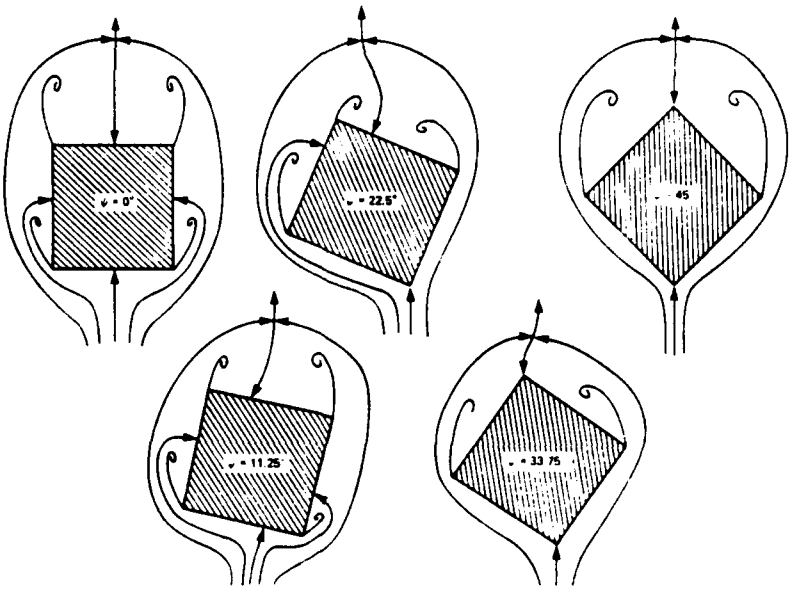

Figure 8. Effect of Roll Angle on the Cross-Flow Topology (No Secondary Separations Shown)

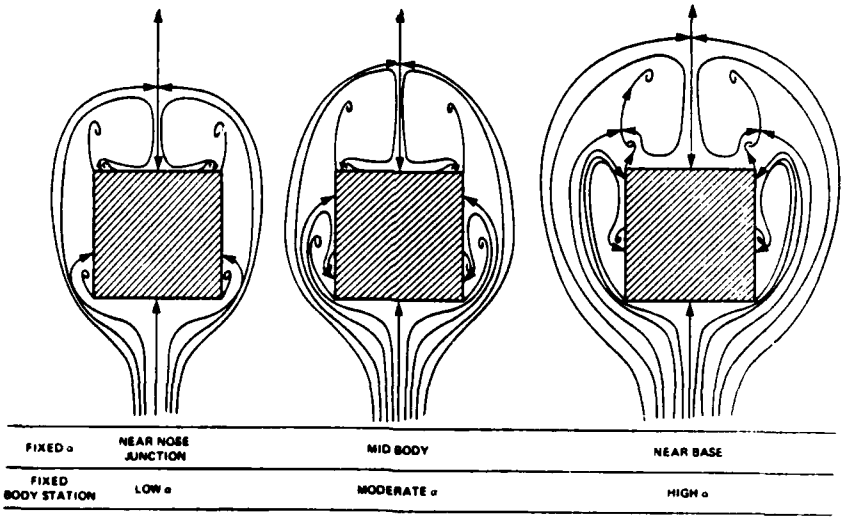

Figure 9. Development of Cross-Flow Topography on a Square Body With Sharp Corners; $\phi = 0°$

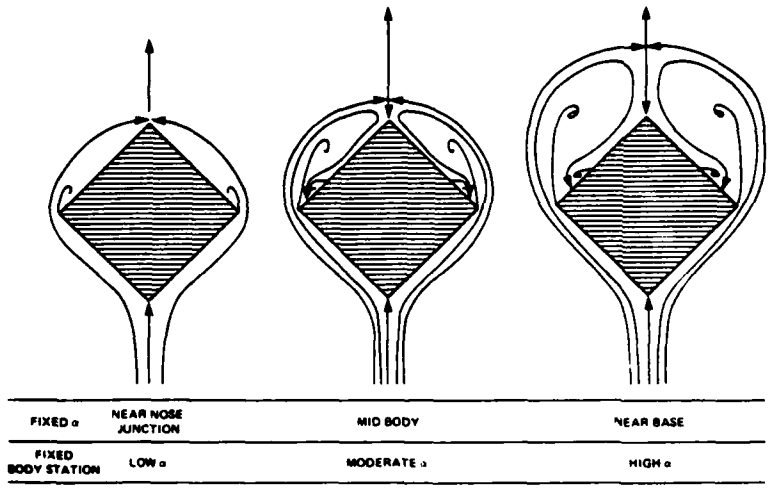

Figure 10. Development of Cross-Flow Topology on a Square Body With Sharp Corners; $\psi = 45°$

Figure 11. Cross-Flow Visualization on an Impulsively Started Cylinder, $\phi = 22\frac{1}{2}°$ After Traveling Several Body Widths

Figure 12. Cross-Flow Visualization on an Impulsively Started Cylinder, $\phi = 45°$ After Traveling Several Body Widths

Figure 13. Cross-Flow Visualization of Model I at α = 45°. Top view is near nose tangency point and bottom view is near mid-model.

To show more detail, Figures 14, 15, and 16 have been included. Figure 14 shows Model III at $\sigma = 15°$ and $\psi = 33°$, and Figure 15 shows the same model at $\sigma = 25°$ and $\psi = 22.5°$. Figure 16 shows Model I at $\sigma = 60°$ and $\psi = 0°$. The double vortex pair that forms at $\psi = 0°$ in the angle of attack range of 14° to 60° is clearly shown.

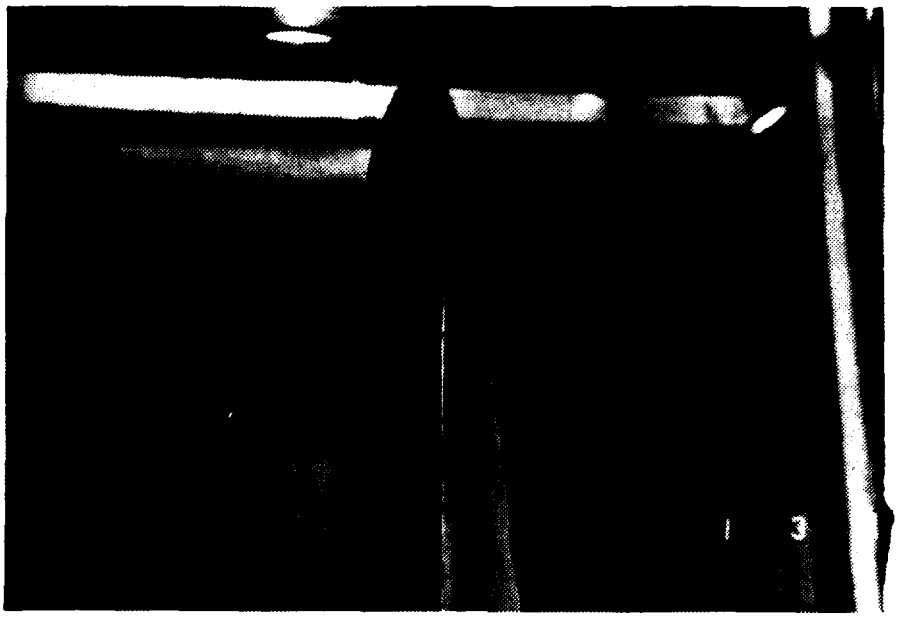

Figure 14. Model III at σ = 15°, ψ = 33°

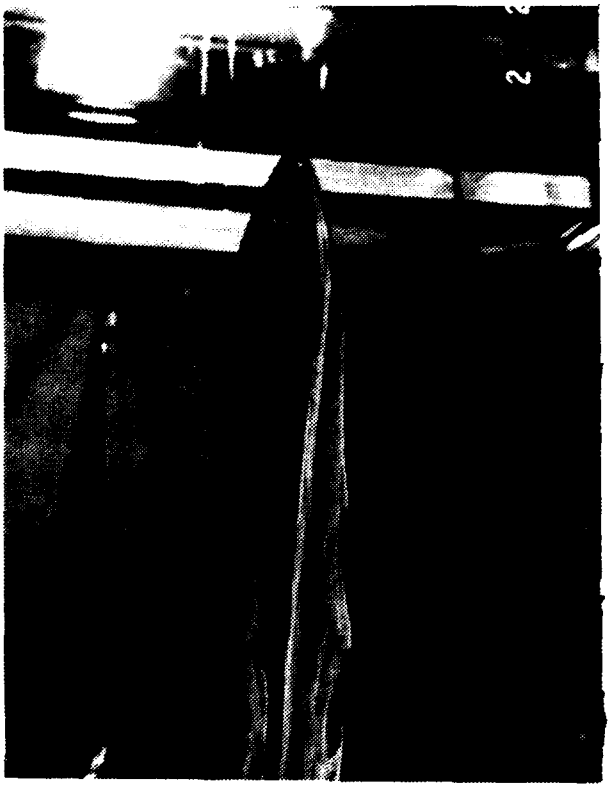

Figure 15. Model III at σ = 25°, ψ = 22½°

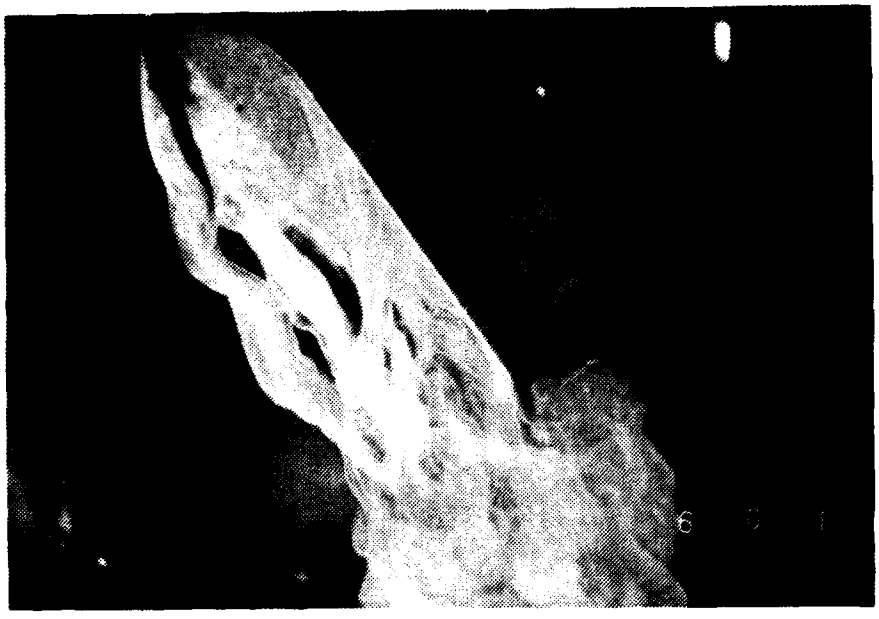

Figure 16. Model I at $\sigma = 60°$, $\psi = 0°$

SECTION V

CONCLUSIONS

Experiments performed on a 4.5-inch sphere in the water tunnel at a Reynolds number of 2600 show separation occurring about as far aft of the meridian as it does ahead of the meridian at Reynolds numbers of 30,000.

It has also been observed that the flow separates near the tangency point on a hemisphere-cylinder at Reynolds numbers of the order of 200,000 but not in the water tunnel at Reynolds numbers of 2000. This is believed due to the strong viscous forces compared to inertia forces at these low Reynolds numbers (Stokes flow). The net result is that the separation lines in the water tunnel are more likely to correspond to turbulent flow than laminar flow. In any case, the primary vortex patterns are likely to be representative of full-scale flight.

REFERENCES

1. Prandtl and Tietjens, "Applied Hydro-and Aeromechanics," McGraw-Hill, 1934.

2. Norton, Brook, "Crossflow Visualization Studies of Bodies at High Angles of Attack," AIAA Student Paper Conference, Southeastern Region, April 1983.

3. Allen, H. J. and Perkins E. W., "Characteristics of Flow over Inclined Bodies of Revolution," NACA RM A50L07, 1950.

4. Yechout, T. R., Zollars, G. J., and Daniel, D. C., "Experimental Aerodynamic Characteristics of Missiles with Square Cross Sections," AIAA Aerospace Sciences Meeting, Paper No. 81-0144, St Louis, Mo, January 12-15, 1981.

5. Lijewski, L. E., Zollars, G. J., Yechout, T. R., and Haupt, B. F., "Experimental Flow Field Measurements of Missiles with Square Cross Sections," AIAA Aerospace Sciences Meeting, Paper No. 82-0055, Orlando Fl, January 11-14, 1982.

6. Daniel, D. C. , Lijewski, L. E., and Zollars, G. J., "Experimental Aerodynamic Studies of Missiles with Square Cross Sections," AGARD-CCP-336, Proceedings from the AGARD Fluid Dynamics Panel Symposium on "Missile Aerodynamics," Trondheim, Norway, September 20-22, 1982.

7. Brittain, V. A., "A Study of Flow Separation Using a Continuous Distribution of Dye Sources," Master's Thesis, University of Florida, Gainsville, Florida, 1981.

8. Clarkson, M. H., Malcolm, G. N., Brittain, V. A. and Intemann, P. A., "Aerodynamic Characteristics of Bodies with Non-Circular Cross Sections at High Angles of Attack," NASA Data Report to be published, 1983.

9. Chapman, G. T., and Clarkson, M. H., "Flow Visualization Studies of Bodies with Square Cross Sections," AIAA Journal, Paper No. 83-0563, January, 1981.

END

FILMED